2011 International Workshop on ADC Modelling, Testing and Data Converter Analysis and Design and IEEE 2011 ADC Forum
June 30 - July 1, 2011. Orvieto, Italy.

A Low-Complexity Adaptive-Threshold Detector for Pulse UWB Systems

D. Strömberg, A. De Angelis, P. Händel

ACCESS Linnaeus Center, Signal Processing Lab, KTH Royal Institute of Technology, Stockholm, Sweden.
phone: +46 8 790 7246, e-mail: {dinos, ales, ph}@kth.se

Abstract - A method for adaptively setting the threshold of an energy detector for Ultra-Wideband radio systems is presented in this paper. The method, which is suitable for low-complexity and low-cost implementation, is based on the estimation of the input noise and interference power. Simulations and experimental results obtained from a prototype UWB system show that the proposed method can adaptively set the threshold of the detector. Therefore it is robust to changes in the interference power, and it can limit the false alarm rate.

I. Introduction

Wireless technology has made it possible to be connected to many different services anywhere when needed. Applications such as mobile phones, digital video broadcast and global positioning via radio transmission have revolutionized the ease of obtaining information about weather, news and location. Today, systems that provide information about our location are becoming a part of our daily lives. Most hand-held mobile units contain a GPS receiver and/or other means, like WLAN positioning, for finding the users location. As people currently spend about 90% of their time indoors [1] indoor positioning systems have become an interesting research topic. The so called Ultra-Wideband (UWB) radio positioning systems has become an intense area of research due to their well fit properties for indoor radio positioning [2].

There are several different design aspects when considering a UWB positioning system, for example: signaling (pulse based or spread spectrum) and complexity of the receiver (coherent or non-coherent). One of the main challenges related to pulse-based UWB systems is the design of the pulse detector [3]. Among the possible detection strategies, the non-coherent energy detection (ED) approach is widely studied in the literature. Its main advantages are low-complexity and low-power implementation, since it avoids Nyquist-rate sampling of the UWB signal, which is infeasible for many applications due to the high bandwidth [4] [5].

This paper presents the evaluation of a low-complexity technique for adaptively setting the threshold of an ED receiver for UWB radio signals. The main goal of the technique is to limit the probability of false detection, or probability of false alarm, in the receiver. This is a fundamental detection theory issue, with a wide range of applications [6]. In particular, concerning the UWB field, a technique based on Cell-Averaging Constant False Alarm Rate (CA-CFAR), derived from radar systems [7], has been studied in [8] in the context of UWB non-coherent signal detection.

Following a similar approach as CA-CFAR, the threshold-setting technique proposed in the present paper is based on an estimate of the noise and interference power at the receiver, obtained during time periods in which no UWB pulse is transmitted. Such power estimation time periods may be scheduled in an operational system by means of a protocol, e.g. an extension of the simple on-off keying addressing scheme previously presented in [9].

The proposed technique is evaluated by means of numerical simulations and by characterizing its performance in an experimental setup. In particular, it is implemented and tested using an evolution of the in-house UWB pulse radio platform prototype for ranging and positioning described in [9], [10] and [11]. This low-cost platform is capable of accurately measuring the round trip time of a pulse propagating between two transceivers, using a time-to-digital converter (TDC) integrated circuit. The particular platform evolution described in the present paper, in the following Section, adds the capability of dynamically adjusting the threshold of the ED UWB receiver.

The remainder of this paper is organized as follows. First, the architecture of the considered UWB system is presented in Section II. Then, in Section III, the proposed adaptive threshold method is derived. Furthermore, an evaluation of the proposed method is presented in Section IV, both by simulations and by implementation on the experimental system. Finally, Section V draws conclusions.

II. System Architecture

The realized custom data acquisition system measures the Round-Trip Time (RTT) of UWB pulses propagating between a master unit and several active responders, indicated as slaves. If the slaves are placed in known

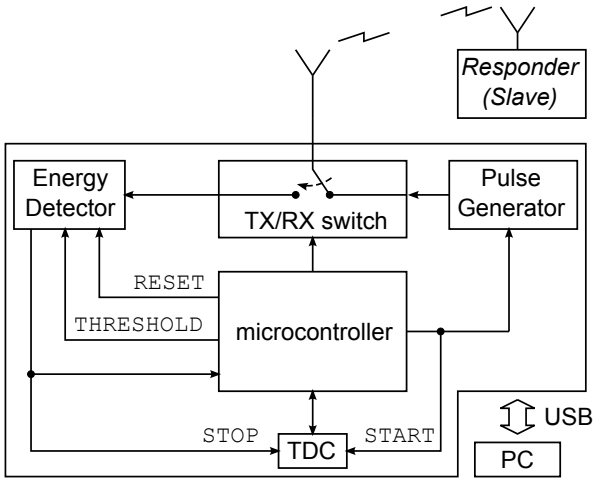

Fig. 1: System architecture block diagram.

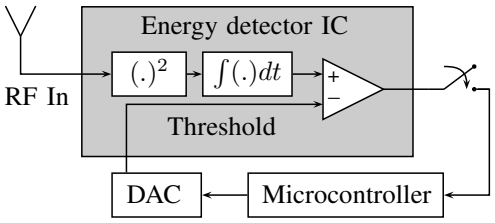

Fig. 2: Adaptive-threshold energy detector implementation. Hardware architecture simplified block diagram.

positions, the master is capable of self-localization. A block diagram of the particular platform evolution analyzed in the present paper is shown in Fig. 1. The main differences with respect to the architecture presented in [9] are the capability of being dynamically reconfigurable as a master or a slave, the use of a single antenna with a switch for both transmission and reception of pulses, the support for adaptive threshold and an improved custom data acquisition and transmission section. In the following, a more detailed description of the main blocks of the architecture in Fig.1 is provided.

The pulse generator block is based on a step recovery diode, providing a pulse of approximately 1 ns width and 9 V amplitude on a 50 Ω load [12]. For both transmission and reception of the pulse, a discone antenna is employed, due to its wide bandwidth and omnidirectional radiation pattern in the horizontal plane. Furthermore, as a fundamental block, in order to perform accurate measurements of the RTT, a TDC commercial integrated circuit is employed, which provides an accuracy of 50 ps. The ”start” logic signal to the TDC is provided by the pulse generator block and corresponds to the time instant in which the pulse is transmitted. On the other hand, the ”stop” signal is provided by the energy detector block, and it corresponds to the time instant in which the response pulse is received. Furthermore, the control and timing operations are implemented by means of a low-power 8-bit microcontroller, programmed in C language. The microcontroller is also used to transmit data to a host Personal Computer via a Universal Serial Bus interface. All processing of the acquired raw RTT data is then implemented in Matlab in the host computer.

A crucial block, with respect to the analysis presented in this paper, is the pulse receiver, which is based on the energy detector approach. For low cost systems the energy detector receiver is implemented directly in analog hardware, thus yielding a low-complexity and low-power implementation, since it avoids sampling the UWB signal at the Nyquist-rate. A more detailed block diagram of the energy detector block is shown in Fig. 2. The characteristics of a diode are used to approximate the squaring operation and an integrator filter is used for the integration operation. The analog output voltage from this circuit will be proportional to the power of the signal at its input terminals. An analog comparator is connected to the output of the energy detector circuit. Furthermore, a Digital to Analog Converter (DAC) is used to set the voltage level, corresponding to the comparator threshold, which has to be crossed for a detection to occur [7]. In [8] it was concluded that knowledge of the noise level is needed to set the threshold and limit the number of errors in the receiver. In the following Section, we describe our proposed method to adaptively set the threshold for this particular energy detection implementation.

III. Proposed adaptive threshold method

The objective is to estimate the received signal power, assumed constant and denoted as $\bar{P}$, when only noise is present at the receiver. The estimation is based on the measured output of the ED at time step k, denoted as $\tilde{P}_k$. This signal is proportional to the received power, averaged over the integration window of the ED. It is assumed that $\tilde{P}_k$ is a sequence of independent identically distributed Gaussian random variables, with mean $\bar{P}$ and variance σ_P^2. Furthermore, we assume that σ_P^2 is sufficiently small such that $Pr\{\tilde{P}_k < 0\}$ is negligible, since a negative power has no physical meaning.

To obtain an estimate of the received signal power, denoted as $\hat{P}_k$, we start by defining the error signal as

$$e_k = \tilde{P}_k - \hat{P}_k \,. \tag{1}$$

A cost function that will show to be useful for the low cost system in [9] is the absolute value of the error. The cost function is given by

$$\mathrm{C}(e_k) = \mathrm{E}\left\{|e_k|\right\} = \mathrm{E}\left\{|\tilde{P}_k - \hat{P}_k|\right\} \tag{2}$$

where $\mathrm{E}\{.\}$ denotes the statistical expectation operator. The power estimation problem is then formulated as an unconstrained optimization problem of the form

$$\min_{\hat{P}_k} \ \mathrm{E}\left\{|\tilde{P}_k - \hat{P}_k|\right\}. \tag{3}$$

The algorithm that solves this problem in an approximate manner is based on the steepest descent method [13] for estimating the noise power. This algorithm solves the noise estimation problem recursively and is robust to changes in the noise power. The formulation of the steepest descent algorithm, with an arbitrary cost function $\mathrm{C}(e_k)$ is

$$\hat{P}_{k+1} = \hat{P}_k - \mu_k \cdot \frac{\partial}{\partial \hat{P}_k} \mathrm{C}(e_k) \tag{4}$$

with the initial condition $\hat{P}_0 \geq 0$. The step size μ_k might be a constant or time-varying quantity. Inserting a cost function of the absolute value type in (2) into (4) yields a so called Least Mean Absolute Error (LMA) algorithm. This algorithm is also called the sign-LMS in the literature [13]. The derivative in (4) is, by using the linearity of the statistical expectation operator, developed to be

$$\frac{\partial}{\partial \hat{P}_k} \ \mathrm{C}(e_k) = E\left\{\frac{\partial}{\partial \hat{P}_k} \ |\tilde{P}_k - \hat{P}_k|\right\} = E\left\{-\mathrm{sgn}(\tilde{P}_k - \hat{P}_k)\right\} \,, \tag{5}$$

where $\mathrm{sgn}(\cdot)$ denotes the sign operator, defined as follows:

$$\mathrm{sgn}(x) = \begin{cases} +1, & \text{if } x > 0 \\ -1, & \text{if } x < 0 \\ 0, & \text{if } x = 0 \end{cases} .$$

The sign of the error at the k:th sample is denoted as

$$S_k = \mathrm{sgn}(\tilde{P}_k - \hat{P}_k). \tag{6}$$

By substituting (6) and (5) in (4), the general recursive steepest descent solution to the power estimation problem becomes

$$\hat{P}_{k+1} = \hat{P}_k + \mu_k \cdot \mathrm{E}\left\{S_k\right\}. \tag{7}$$

The statistical expectation operator in (7) can be approximated in several ways in analogy with the Least Mean Squares (LMS) theory [13]. One approach is to approximate the expected value of the cost function by the sample mean of the sign of the observed instantaneous errors samples. This can be done in several ways. In the case where all the observed sign samples are used in the sample mean, the *smoothed sign* LMA algorithm is obtained, which follows

$$\hat{P}_{k+1} = \hat{P}_k + \mu_k \cdot \frac{1}{k+1} \sum_{n=0}^{k} S_n. \tag{8}$$

Computing the sample mean of all previous samples, in a growing data set, is not efficient from a computational complexity point of view. To improve the computational complexity of the algorithm it is possible to instead use the N most recent samples of the sign of the instantaneous errors, this yields the so called *moving window sign* LMA algorithm, which is

$$\hat{P}_{k+1} = \hat{P}_k + \mu_k \cdot \frac{1}{N} \sum_{n=k-N+1}^{k} S_n. \tag{9}$$

This sets a bound on the number of samples that have to be stored in the memory. Another standard method used in the LMS theory is to approximate the statistical expectation value by the current instantaneous error sample, which is equivalent to setting $N = 1$ in (9). The recursive solution if the latest sign sample is used is called the *instantaneous sign* LMA algorithm, this algorithm is

$$\hat{P}_{k+1} = \hat{P}_k + \mu_k \cdot S_k. \tag{10}$$

As stated before, the step size μ_k in the algorithms (8), (9) and (10) might be a constant or time-varying step size. The latter variant may be used to accelerate the convergence and to allow fast tracking if the received power changes over time. In particular, using intuitive reasoning, a good criterion for changing the step size is that the algorithm has not yet crossed the measured power level $\tilde{P}_k$. In this case the step size should be *increased* to accelerate the convergence. Conversely, if the algorithm has crossed $\tilde{P}_k$, the step size should be *decreased*, in order to improve the estimation accuracy in further iterations. The variable step size has been adjusted in a multiplicative manner, with the scaling factor δ and the following criterion:

$$\mu_{k+1} = \begin{cases} \mu_k \cdot \delta, & \text{if } S_k = S_{k-1} \\ \frac{\mu_k}{\delta}, & \text{if } S_k \neq S_{k-1} \end{cases} . \tag{11}$$

A general flow-chart of the algorithm is shown in Fig. 3.

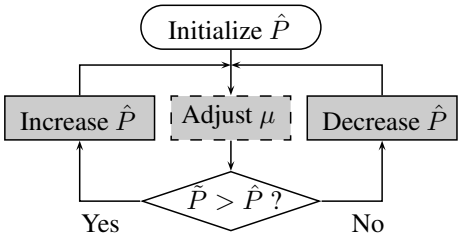

Fig. 3: Adaptive-threshold algorithm flowchart, dotted lines correspond to optional step in the time-variant step-size version.

In the hardware implementation, a comparator with a voltage-controlled threshold is connected to the output of the ED, as shown in the block diagram of Fig. 2. This configuration allows to obtain the quantity S_k, which is related to the decided hypotheses, in a straightforward manner at the output of the comparator, since the threshold voltage is proportional to $\hat{P}_k$. The decided hypotheses can be used as a feedback to control the false alarm rate through the threshold. The algorithms in (8) - (10) hence apply directly to the hardware and may be programmed into the microcontroller.

IV. Evaluation

The algorithm in (10) has been selected for implementation in the hardware platform, because it requires the least amount of memory and provides the fastest convergence time among the ones tested in simulation. In the following subsections, we show results from simulation and experimental characterization related to this algorithm.

A. Simulations

To measure the performance of the algorithm, the so called *misalignment* Δ_k of the LMA algorithm is used, defined as

$$\Delta_k = |P - \hat{P}_k| , \tag{12}$$

where P is the true noise power, which is known (set by the program) in the simulations. The instantaneous sign LMA algorithm has been simulated in white Gaussian noise with a constant power of $P = 0.01\ W$. The integrator time constant is 1 μs and a sampling frequency of 10 MHz has been used for the output of the energy detector. The estimated power $\hat{P}_k$ as a function of time is shown in Fig. 4(a), while the absolute error (misalignment) is shown in Fig. 4(b). Another important performance measure of these algorithms is the time it takes for the estimate to reach a steady state, also known as convergence time. The convergence time, in samples, may be calculated for an algorithm that converges to a steady state value with the following *stopping criterion*

$$\Delta_k < \frac{\rho \cdot P}{100} , \tag{13}$$

where ρ is given in percent. In other words, the time index of the first sample that has an error within ρ % of the true noise power is considered to be the convergence time. The convergence time (in samples) is obtained

from the following *selection rule*, which selects the first sample that fulfills the stopping criterion

$$\arg\min_k \left\{ \Delta_k < \frac{\rho \cdot P}{100} \right\}. \tag{14}$$

Both the variants of the algorithm provide an accurate estimation of the power, with a steady-state error of less than 0.001 W. However, the variable step size version is faster, reaching convergence in about 40% of the time compared to the constant step size variant, as shown in Fig. 4(a) and 4(b).

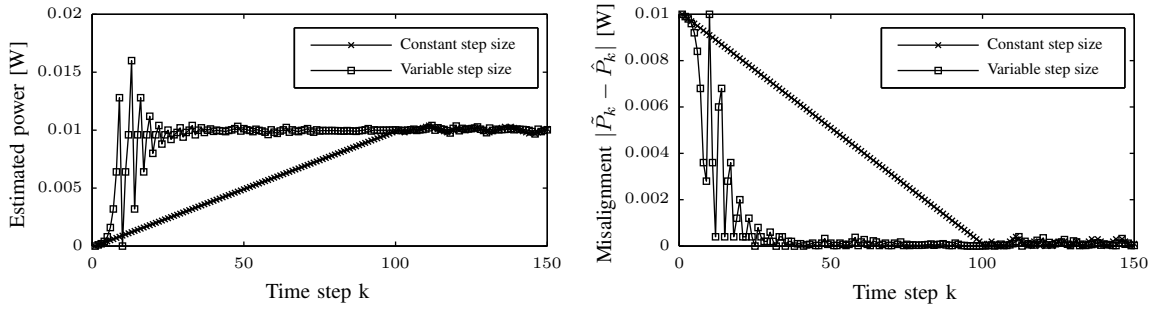

Fig. 4: Simulation results. (a) Operation of the algorithm over time. (b) Algorithm's misalignment over time.

In the following section we show that the experimental results are in good agreement with the simulations.

B. Experimental results

The experimental tests on the platform have been conducted using an omnidirectional UWB receiver antenna in a controlled environment, with a low constant level of noise and external interference. To investigate the adaptive capabilities of the system, an UWB pulse transmitter, described in [11], was placed in line-of-sight at a distance of 1 m from the receiver antenna. During the test, the transmitter was initially disabled, and then switched on, thus transmitting pulses at a pulse-repetition rate of about 1 KHz. The sampling frequency at the receiver was about 60 Hz. The results are shown in Fig. 5(a) and 5(b), and validate the ability to track sudden changes in the received power.

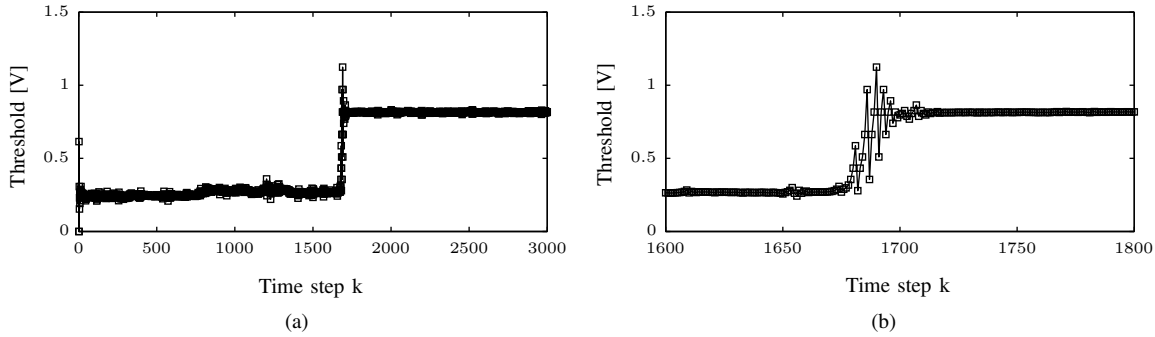

Fig. 5: Experimental results. (a) Behavior of the threshold over time. (b) Magnification of the change in received power level, corresponding to the time interval during which the transmitter was switched on.

Furthermore, in order to provide an empirical analysis of the false alarm rate, an additional measurement experiment has been performed as follows. The receiver was placed in a controlled lab indoor environment and no pulse was transmitted, thus only noise and interference were present. An estimate of the noise power $\hat{P}_0$ was obtained by averaging 1000 values provided by the developed algorithm in (10), after it had reached convergence. Subsequently, the threshold $\hat{P}$ of the comparator was set according to the following relation:

$$\hat{P} = M \cdot \hat{P}_0, \tag{15}$$

where M is a constant hereby referred to as the *threshold multiplier*. The value of M has been sequentially set from 0.95 to 1.05 at 0.0025 steps. For each step, a predefined number $N = 1000$ of samples of the comparator output has been acquired. The number of detections observed for a given M is denoted as $N_D(M)$. Finally, the empirical false alarm rate $p_{FA}(M)$ is calculated as

$$p_{FA}(M) = \frac{N_D(M)}{N}. \tag{16}$$

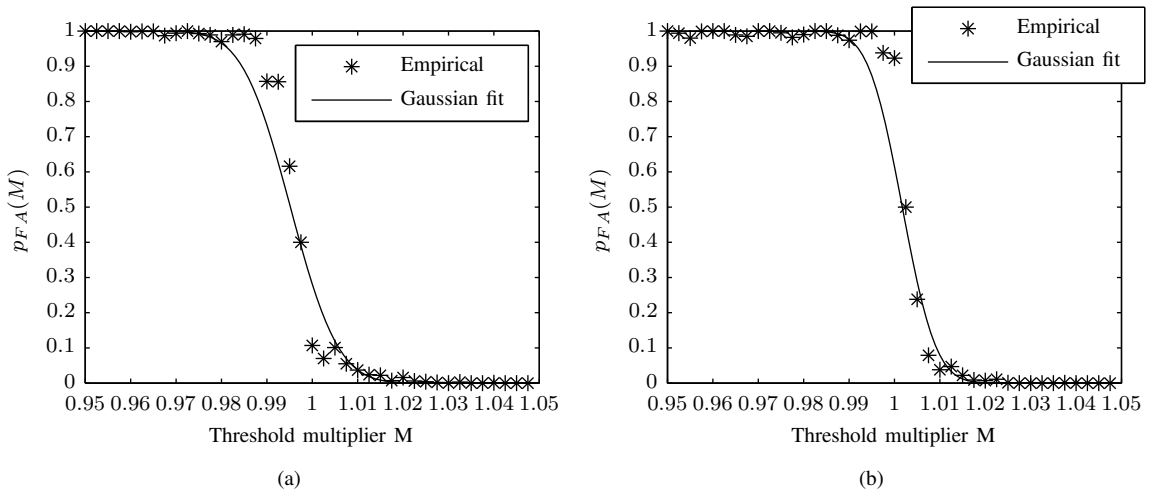

Fig. 6: Empirical false alarm probability vs threshold multiplier, (a) discone antenna, (b) commercial wideband antenna.

The results of this experiment are shown in Figures 6(a) and 6(b), for an in-house developed wideband discone antenna and a commercial wideband antenna, respectively. Such empirical curves are useful to establish the optimal M which has to be used to obtain a desired false alarm probability. As an example, from Fig. 6(a) we can see that a negligible false alarm rate is obtained with a threshold multiplier of 1.05, which is 5% higher than the estimated noise.

V. Conclusion

The results show that the proposed method, in the variable step-size version, is able to quickly and accurately track changes in received power, in accordance with the simulations. The proposed technique is suitable for implementation in low-complexity and low-cost systems, since it relies on a simple architecture: an energy-detector followed by a comparator. Further, the technique readily provides a measure of the received signal strength, which could be integrated with time-of-arrival measurements to improve the ranging accuracy and integrity. The decided hypotheses can be used as a feedback to control the false alarm rate by adjusting the threshold when noise is only present at the energy detector input.

References

[1] US Environmental Protection Agency, "The inside story: A guide to indoor air quality.," December 2010. http://www.epa.gov/iaq/pubs/insidest.html.
[2] S. Gezici, Z. Tian, G. Giannakis, H. Kobayashi, A. Molisch, H. Poor, and Z. Sahinoglu, "Localization via ultra-wideband radios: a look at positioning aspects for future sensor networks," *IEEE Signal Processing Magazine*, vol. 22, pp. 70–84, July 2005.
[3] Z. Sahinoglu, S. Gezici, and S. Güvenc, *Ultra-wideband Positioning Systems*. Cambridge University Press, 2008.
[4] D. Dardari, A. Conti, U. Ferner, A. Giorgetti, and M. Win, "Ranging with ultrawide bandwidth signals in multipath environments," *Proceedings of the IEEE*, vol. 97, no. 2, pp. 404 –426, 2009.
[5] A. Mariani, A. Giorgetti, and M. Chiani, "Energy detector design for cognitive radio applications," in *Waveform Diversity and Design Conference (WDD), 2010 International*, pp. 53 –57, 2010.
[6] S. M. Kay, *Fundamentals of statistical signal processing. Vol. 2, Detection theory*. Upper Saddle River, N.J.: Prentice Hall PTR, 1998.
[7] B. R. Mahafza, *Radar systems analysis and design using MATLAB*. Boca Raton: Chapman & Hall/CRC, 2nd ed., 2005.
[8] A. Maali, A. Mesloub, M. Djeddou, H. Mimoun, G. Baudoin, and A. Ouldali, "Adaptive ca-cfar threshold for non-coherent ir-uwb energy detector receivers," *Communications Letters, IEEE*, vol. 13, pp. 959 –961, december 2009.
[9] A. De Angelis, J. Nilsson, I. Skog, P. Händel, and P. Carbone, "Indoor Positioning by Ultrawide Band Radio Aided Inertial Navigation," *Metrology and Measurement Systems*, vol. 17, no. 3, pp. 447–460, 2010.
[10] A. De Angelis, M. Dionigi, R. Moschitta, A. Giglietti, and P. Carbone, "Characterization and Modeling of an Experimental UWB Pulse-Based Distance Measurement System," *IEEE Transactions on Instrumentation and Measurement*, vol. 58, pp. 1479 – 1486, May 2009.
[11] A. De Angelis, A. Moschitta, P. Händel, and P. Carbone, *Advances in Measurement Systems*, ch. Experimental Radio Indoor Positioning Systems Based on Round-Trip Time Measurement. INTECH (publ.), Available from: http://sciyo.com, 2010.
[12] A. De Angelis, M. Dionigi, R. Giglietti, and P. Carbone, "Experimental comparison of low-cost sub-nanosecond pulse generators," *IEEE Transactions on Instrumentation and Measurement*, vol. 60, pp. 310 –318, jan. 2011.
[13] A. H. Sayed, *Fundamentals of adaptive filtering*. Hoboken, N.J.: Wiley, 2003.